Published for SISSA by Springer

Received: August 19, 2023
Revised: January 26, 2024
Accepted: April 22, 2024
Published: May 16, 2024

Explanation of the hints for a 95 GeV Higgs boson within a 2-Higgs Doublet Model

A. Belyaev[a,b] **R. Benbrik**[c] **M. Boukidi**[c] **M. Chakraborti**[a] **S. Moretti**[a,d] **and S. Semlali**[a,b]

[a] *School of Physics and Astronomy, University of Southampton, Southampton, SO17 1BJ, United Kingdom*
[b] *Particle Physics Department, Rutherford Appleton Laboratory, Chilton, Didcot, Oxon OX11 0QX, United Kingdom*
[c] *Polydisciplinary Faculty, Laboratory of Fundamental and Applied Physics, Cadi Ayyad University, Sidi Bouzid, B.P. 4162, Safi, Morocco*
[d] *Department of Physics and Astronomy, Uppsala University, Box 516, SE-751 20 Uppsala, Sweden*

E-mail: a.belyaev@soton.ac.uk, r.benbrik@uca.ac.ma, mohammed.boukidi@ced.uca.ma, mani.chakraborti@gmail.com, s.moretti@soton.ac.uk, s.semlali@soton.ac.uk

Abstract: We suggest an explanation for and explore the consequences of the excess around 95 GeV in the di-photon and di-tau invariant mass distributions recently reported by the CMS collaboration at the Large Hadron Collider (LHC), together with the discrepancy that has long been observed at the Large Electron-Positron (LEP) collider in the $b\bar{b}$ invariant mass. Interestingly, the most recent findings announced by the ATLAS collaboration do not contradict, or even support, these intriguing observations. Their search in the di-photon final state similarly reveals an excess of events within the same mass range, albeit with a bit lower significance, thereby corroborating and somewhat reinforcing the observations made by CMS.

We demonstrate that the lightest CP-even Higgs boson in the general 2-Higgs Doublet Model (2HDM) Type-III can explain simultaneously the observed excesses at approximately 1.3 σ C.L. while satisfying up-to-date theoretical and experimental constraints. Moreover, the 2HDM Type-III predicts an excess in the $pp \to t\bar{t}H_{\rm SM}$ production channel of the 125 GeV Higgs boson, $H_{\rm SM}$. This effect is caused by a up to 12% enhancement of the $H_{\rm SM}tt$ Yukawa coupling in comparison to that predicted by the Standard Model. Such an effect can be tested at the High Luminosity LHC (HL-LHC), which can either discover or exclude the scenario we suggest. This unique characteristic of the 2HDM Type-III makes this scenario with the 95 GeV resonance very attractive for further theoretical and experimental investigations at the (HL-)LHC and future colliders.

Keywords: Higgs Production, New Light Particles

ArXiv ePrint: 2306.09029

https://doi.org/10.1007/JHEP05(2024)209

Contents

1 Introduction

In the last ten years, a great amount of effort has been put into the precise determination of the properties of the Higgs boson, following its discovery at the Large Hadron Collider (LHC) in 2012 [1, 2]. Many such properties are now established with accuracies better than 10% and most of the experimental observations made up to date are consistent with the Standard Model (SM) expectations. Nevertheless, current precision Higgs physics at the LHC provides room for the possibility to go Beyond the SM (BSM) in search of additional Higgs states besides the SM-like one, with masses ranging from a few GeV up to the TeV scale. Many well-motivated BSM scenarios with extended Higgs sectors, either fundamental (e.g., various Supersymmetric models [3]) or effective ones (e.g., 2-Higgs Doublet Models (2HDMs) [4, 5]), predict the existence of extra light and heavy Higgs bosons, thus motivating searches for these non-standard (pseudo)scalar states at various lepton and hadron colliders.

The 2HDM is one of the most well-studied BSM scenarios where the SM Higgs sector is extended by one additional Higgs doublet. In the most generic version of the 2HDM, the Yukawa couplings are non-diagonal in flavour space since each of the two Higgs doublets couple to all the SM fermions simultaneously. As a consequence, unwanted tree-level Flavour Changing Neutral Currents (FCNCs) may be induced, contradicting experimental observations. To tackle this problem, usually a Z_2 symmetry is imposed on the model that determines in turn the coupling structure of the two Higgs doublets to the SM fermions, so that the 2HDM can be classified into the so-called Type-I, Type-II, lepton-specific and flipped scenarios [5]. However, there is another possibility, i.e., the 2HDM Type-III where, instead of introducing such a Z_2 symmetry, one allows for simultaneous couplings of the two Higgs doublets to all SM fermions. The generic Yukawa structure resulting from such a configuration can be constrained using various theoretical requirements of self-consistency of the model as well as a range of experimental measurements of the Higgs masses and couplings present in the model.

JHEP05(2024)209

In the ongoing search for a low-mass Higgs boson, the CMS collaboration reported in 2018 an excess in the invariant mass of di-photon events near 95 GeV [6]. In March 2023, CMS has released their latest results, confirming the excess by employing advanced analysis techniques and utilising data collected during the first, second and third years of Run 2, corresponding to integrated luminosities of 36.3 fb^{-1}, 41.5 fb^{-1} and 54.4 fb^{-1}, respectively, all at a center-of-mass energy of 13 TeV [7]. The combined data exhibited an excess with a local significance of 2.9σ at a mass of $m_{\gamma\gamma} = 95.4\,\text{GeV}$.

The ATLAS collaboration recently released their findings in this channel derived from the full Run 2 data set [8]. Notably, their latest analysis showcases a significantly enhanced level of sensitivity compared to their previous study, which relied on only 80 fb^{-1} of data [9]. In their updated analysis, ATLAS reveals an excess with a local significance of 1.7σ in the $\gamma\gamma$ channel around an invariant mass of 95 GeV, remarkably aligning with the reported CMS observation.

Furthermore, an additional excess has recently been reported by CMS in the search for a light neutral (pseudo)scalar boson ϕ in the production and decay process $gg,\, b\bar{b} \to \phi \to \tau\tau$ [10], with a local (global) significance of $3.1\sigma(2.7\sigma)$ for $m_\phi \approx 100$ GeV. Considering the poor resolution of $m_{\tau\tau}$ in comparison to $m_{\gamma\gamma}$, the two excesses observed in the two final states actually appear to be compatible. Previously, the Large Electron Positron (LEP) collider collaborations [11] explored the low-mass domain extensively in the $e^+e^- \to Z\phi$ production mode, with a generic Higgs boson state ϕ decaying via the $\tau\tau$ and $b\bar{b}$ channels. Interestingly, an excess has been reported in 2006 in the $e^+e^- \to Z\phi(\to b\bar{b})$ mode for $m_{b\bar{b}}$ around 98 GeV [12]. Given the limited mass resolution of the di-jet invariant mass at LEP, this anomaly may well coincide with the aforementioned excesses seen by CMS and/or ATLAS in the $\gamma\gamma$ and $\tau\tau$ final state. Since the excesses appear in very similar mass regions, several studies [13–29] have explored the possibility of simultaneously explaining these anomalies within BSM frameworks featuring a non-standard Higgs state lighter than 125 GeV, while being in agreement with current measurements of the properties of the ≈ 125 GeV SM-like Higgs state observed at the LHC. In the attempt to explain the excesses in the $\gamma\gamma$ and $b\bar{b}$ channels, it was found in refs. [30, 31] that the 2HDM Type-III with a particular Yukawa texture can successfully accommodate both measurements simultaneously with the lightest CP-even Higgs boson of the model, while being consistent with all relevant theoretical and experimental constraints. Further recent studies have shown that actually all three aforementioned signatures can be simultaneously explained in the 2HDM plus a real (N2HDM) [26] and complex (S2HDM) [27, 29] singlet.

In our study, we show that all three anomalies seen in the $\gamma\gamma$, $\tau\tau$ and $b\bar{b}$ final states can also be explained within the 2HDM Type-III of refs. [30, 31], at approximately 1.3 σ C.L. thereby making the point that one does not need to go beyond the minimal 2HDM framework. Moreover, in our study, we have found an important prediction. The parameter space of 2HDM Type-III explaining the anomalous data, predicts an enhancement of $H_{\text{SM}}tt$ Yukawa coupling and the respective uplift of the $gg, q\bar{q} \to t\bar{t}H_{\text{SM}}$ production of the SM-like Higgs, which can be tested in the near future to discover or exclude the scenario we suggest.

The paper is organised as follows. In section 2, we review the theoretical framework we have chosen, i.e., the 2HDM Type-III. We describe the three excesses observed at LEP and the LHC in section 3. In section 4, we outline the relevant theoretical and experimental

JHEP05(2024)209

constraints considered in this analysis. In section 5, we present our numerical set-up to scan the parameter space of the 2HDM Type-III in order to find an explanation of the three anomalies and how this can be achieved, including the consequences for other Higgs processes. Finally, we conclude in section 6.

2 2HDM Type-III

The 2HDM includes two $\mathrm{SU}(2)_L$ doublets with hypercharge $Y = 1$. The most general renormalisable $\mathrm{SU}(2)_L \times \mathrm{U}(1)_Y$ invariant scalar potential is written as follows [5]:

$$\begin{aligned}\mathcal{V} = {} & m_{11}^2 \Phi_1^\dagger \Phi_1 + m_{22}^2 \Phi_2^\dagger \Phi_2 - \left[m_{12}^2 \Phi_1^\dagger \Phi_2 + \text{H.c.} \right] + \lambda_1 (\Phi_1^\dagger \Phi_1)^2 + \lambda_2 (\Phi_2^\dagger \Phi_2)^2 + \lambda_3 (\Phi_1^\dagger \Phi_1)(\Phi_2^\dagger \Phi_2) \\ & + \lambda_4 (\Phi_1^\dagger \Phi_2)(\Phi_2^\dagger \Phi_1) + \frac{1}{2} \left[\lambda_5 (\Phi_1^\dagger \Phi_2)^2 + \text{H.c.} \right] + \left\{ \left[\lambda_6 (\Phi_1^\dagger \Phi_1) + \lambda_7 (\Phi_2^\dagger \Phi_2) \right] (\Phi_1^\dagger \Phi_2) + \text{H.c.} \right\},\end{aligned} \tag{2.1}$$

where m_{11}^2, m_{22}^2, m_{12}^2 are mass squared terms and λ_i ($i = 1, \ldots, 7$) are dimensionless quantities describing the coupling of the order-4 interactions. Of all such parameters, 6 are real (m_{11}^2, m_{22}^2 and λ_i with $i = 1, \ldots, 4$) and 4 are a priori complex (m_{12}^2 and λ_i with $i = 5, \ldots, 7$). Therefore, in general, the model has 14 free parameters. Under appropriate manipulations, this number can however be reduced. Following ref. [32], to start with, one can diagonalise the quadratic part of the potential in the (Φ_1, Φ_2) space, removing the m_{12}^2 term, thus getting rid of 2 parameters. Then, one can make a relative U(1) transformation on Φ_1 or Φ_2, making λ_5 real, hence down to 11 parameters. Next, by removing CP violation, the number of free parameters reduces to 9 (this requires making one neutral Higgs state decouple from both VV ($VV = W^+W^-$ and ZZ) and H^+H^- interactions). Furthermore, the Yukawa matrices corresponding to the two doublets are not simultaneously diagonalisable, which can pose a problem, as the off-diagonal elements lead to tree-level Higgs mediated Flavour Changing Neutral Currents (FCNCs) on which severe experimental bounds exist. The Glashow-Weinberg-Paschos (GWP) theorem [33, 34] states that this type of FCNCs is absent if at most one Higgs multiplet is responsible for providing mass to fermions of a given electric charge. This GWP condition can be enforced by a discrete Z_2-symmetry ($\Phi_1 \to +\Phi_1$ and $\Phi_2 \to -\Phi_2$) on the doublets, in which case the absence of FCNCs is natural. However, the need to allow for a softly broken Z_2-symmetry (in turn re-introducing a small m_{12}^2), as customarily done to enable Electro-Weak Symmetry Breaking (EWSB) compliant with experimental measurements, relies on the existence of a basis where $\lambda_6 = \lambda_7 = 0$. As a consequence, altogether, one loses 2 parameters (λ_6 and λ_7) but regains 1 (m_{12}^2), thus reducing further their overall number down to 8.

Then, after EWSB has taken place, each scalar doublet acquires a Vacuum Expectation Value (VEV) that can be parametrised as follows:

$$\langle \Phi_1 \rangle = \frac{v}{\sqrt{2}} \begin{pmatrix} 0 \\ \cos\beta \end{pmatrix} \qquad \langle \Phi_2 \rangle = \frac{v}{\sqrt{2}} \begin{pmatrix} 0 \\ \sin\beta \end{pmatrix}, \tag{2.2}$$

where the angle β determines the ratio of the two doublet VEVs, v_1 and v_2, as $\tan\beta = v_2/v_1$, and where $v = 246\,\text{GeV}$ is a fixed value, thereby giving a final count of 7 free parameters,

JHEP05(2024)209

which we choose to be:

$$m_h, \quad m_H, \quad m_A, \quad m_{H^\pm}, \quad \sin(\beta-\alpha), \quad \tan\beta, \quad m_{12}^2, \tag{2.3}$$

where α is the mixing angle in the CP-even Higgs sector, m_H and m_h denote the two CP-even Higgs masses (with $m_h < m_H$ and where either of these can be the discovered SM-like Higgs state $H_{\rm SM}$,[1]) whereas $m_{H^\pm}$ and m_A are the masses of the charged and CP-odd Higgs states, respectively. (In the remainder, we will use the short-hand notation s_x and c_x in place of $\sin(x)$ and $\cos(x)$.)

In the Yukawa sector, the general scalar to fermions couplings are given by:

$$\begin{aligned} -\mathcal{L}_Y = &\bar{Q}_L Y_1^u U_R \tilde{\Phi}_1 + \bar{Q}_L Y_2^u U_R \tilde{\Phi}_2 + \bar{Q}_L Y_1^d D_R \Phi_1 + \bar{Q}_L Y_2^d D_R \Phi_2 \\ &+ \bar{L} Y_1^\ell \ell_R \Phi_1 + \bar{L} Y_2^\ell \ell_R \Phi_2 + \text{H.c.}, \end{aligned} \tag{2.4}$$

where $Y_{1,2}^f$ are 3×3 Yukawa matrices in flavour space and $\tilde{\Phi}_{1,2} = i\sigma_{1,2}\Phi_{1,2}^*$, with $\sigma_{1,2}$ being the Pauli matrices. After EWSB has taken place, one can then derive the fermion masses from eq. (2.4).

Here, however, we investigate a modified version of the described 2HDM, the so-called Type-III, where neither a global symmetry is implemented in the Yukawa sector nor any alignment in flavour space is enforced. We adopt instead the Cheng-Sher ansatz [35, 36], which assumes a flavour symmetry in turn suggesting a specific texture of the Yukawa matrices, where FCNC effects are proportional to the geometric mean of the two fermion masses and dimensionless parameters[2] χ_{ij}^f ($\propto \sqrt{m_i m_j}/v\ \chi_{ij}^f$), where $i,j = 1-3$. After EWSB, the Yukawa sector can be expressed in terms of the mass eigenstates of the Higgs bosons, as follows:

$$\begin{aligned} -\mathcal{L}_Y^{\rm III} = &\sum_{f=u,d,\ell} \frac{m_j^f}{v} \times \left((\xi_h^f)_{ij} \bar{f}_{Li} f_{Rj} h + (\xi_H^f)_{ij} \bar{f}_{Li} f_{Rj} H - i(\xi_A^f)_{ij} \bar{f}_{Li} f_{Rj} A \right) \\ &+ \frac{\sqrt{2}}{v} \sum_{k=1}^{3} \bar{u}_i \left[\left(m_i^u (\xi_A^{u*})_{ki} V_{kj} P_L + V_{ik} (\xi_A^d)_{kj} m_j^d P_R \right) \right] d_j H^+ \\ &+ \frac{\sqrt{2}}{v} \bar{\nu}_i (\xi_A^\ell)_{ij} m_j^\ell P_R \ell_j H^+ + \text{H.c.}\,, \end{aligned} \tag{2.5}$$

where the $(\xi_\phi^f)_{ij}$ couplings are given in table 1 in terms of the free parameters χ_{ij}^f, $\tan\beta$ and the mixing angle α. These expressions encompass the Higgs-fermion interactions of 2HDM Type-II[3] together with a contribution coming from the Yukawa texture.[4]

Based on the arguments presented above, the fundamental components of the Yukawa sector can be obtained in terms of the χ_{ij}^f parameters. These are additional free parameters of the model which describe masses and mixings of the quarks and leptons. It is crucial to ensure that rare decays, which are suppressed in the SM, do not exceed current bounds, though. Specifically, it is important to investigate the contributions of Higgs bosons to FCNC processes in B mesons. Here, the non-diagonal terms are not considered and the

[1] In our numerical analysis, we will assume $H \equiv H_{\rm SM}$.
[2] We refer the readers to ref. [37] for more details.
[3] The 2HDM Type-II is restored when $\chi_{ij} = 0$.
[4] Here, $\xi_f^{\rm III} = \xi_f^{II} + \Delta_{ij}$, with $\Delta_{ij} \sim \chi_{ij}$ [37, 38].

JHEP05(2024)209

ϕ	$(\xi^u_\phi)_{ij}$	$(\xi^d_\phi)_{ij}$	$(\xi^\ell_\phi)_{ij}$
h	$\frac{c_\alpha}{s_\beta}\delta_{ij} - \frac{c_{\beta-\alpha}}{\sqrt{2}s_\beta}\sqrt{\frac{m^u_i}{m^u_j}}\chi^u_{ij}$	$-\frac{s_\alpha}{c_\beta}\delta_{ij} + \frac{c_{\beta-\alpha}}{\sqrt{2}c_\beta}\sqrt{\frac{m^d_i}{m^d_j}}\chi^d_{ij}$	$-\frac{s_\alpha}{c_\beta}\delta_{ij} + \frac{c_{\beta-\alpha}}{\sqrt{2}c_\beta}\sqrt{\frac{m^\ell_i}{m^\ell_j}}\chi^\ell_{ij}$
H	$\frac{s_\alpha}{s_\beta}\delta_{ij} + \frac{s_{\beta-\alpha}}{\sqrt{2}s_\beta}\sqrt{\frac{m^u_i}{m^u_j}}\chi^u_{ij}$	$\frac{c_\alpha}{c_\beta}\delta_{ij} - \frac{s_{\beta-\alpha}}{\sqrt{2}c_\beta}\sqrt{\frac{m^d_i}{m^d_j}}\chi^d_{ij}$	$\frac{c_\alpha}{c_\beta}\delta_{ij} - \frac{s_{\beta-\alpha}}{\sqrt{2}c_\beta}\sqrt{\frac{m^\ell_i}{m^\ell_j}}\chi^\ell_{ij}$
A	$\frac{1}{t_\beta}\delta_{ij} - \frac{1}{\sqrt{2}s_\beta}\sqrt{\frac{m^u_i}{m^u_j}}\chi^u_{ij}$	$t_\beta\delta_{ij} - \frac{1}{\sqrt{2}c_\beta}\sqrt{\frac{m^d_i}{m^d_j}}\chi^d_{ij}$	$t_\beta\delta_{ij} - \frac{1}{\sqrt{2}c_\beta}\sqrt{\frac{m^\ell_i}{m^\ell_j}}\chi^\ell_{ij}$

Table 1. Yukawa interactions in the 2HDM Type-III.

constraints from $\Delta B = 2$ processes can be ignored due to the suppression factor $\sqrt{m^f_j m^f_i}/v$. However, our analysis takes into account transitions involving $\Delta B = 1$ processes. The loop transition $b \to s\gamma$ is also sensitive to BSM physics, as deviations from the currently measured rate and SM predictions could indicate the presence of a light charged Higgs boson with appropriate Yukawa couplings. Finally, since CP violation is not observed in the lepton sector, it is reasonable to assume that the χ_{ij}'s are real numbers and the ensuing matrix is symmetric. However, the presence of these terms could also modify FCNCs in the Higgs sector, particularly $h \to f_i\bar{f}_j$ processes, which are proportional to non-diagonal matrix terms [36, 39], so corresponding constraints need to be enforced.

In the presence of the χ^f_{ij} texture parameters, alongside the standard 2HDM inputs of eq. (2.3), we will start our analysis by testing the 2HDM Type-III against theoretical and current experimental constraints, which we do in the forthcoming section.

3 The excesses in $h \to \gamma\gamma$, $\tau\tau$ and $b\bar{b}$ channels

In this section, we investigate whether the 2HDM Type-III can describe consistently the excess observed by both LEP and the LHC at 94–100 GeV in the $\gamma\gamma$, $\tau\tau$ and $b\bar{b}$ channels. The evaluation of the so-called 'signal strengths' for these excesses was done in the Narrow Width Approximation (NWA), in terms of the product of the relevant production cross section (σ, which at the LHC is dominated by gluon-gluon fusion through the top-quark loop[5] and at LEP by the Bjorken channel) as well as decay Branching Ratios ($\mathcal{BR}$s) as follows:

$$\mu_{b\bar{b}} = \frac{\sigma_{\rm 2HDM}(e^+e^- \to Z\phi)}{\sigma_{\rm SM}(e^+e^- \to Zh_{\rm SM})} \times \frac{\mathcal{BR}_{\rm 2HDM}(\phi \to b\bar{b})}{\mathcal{BR}_{\rm SM}(h_{\rm SM} \to b\bar{b})} = |c_{\phi ZZ}|^2 \times \frac{\mathcal{BR}_{\rm 2HDM}(\phi \to b\bar{b})}{\mathcal{BR}_{\rm SM}(h_{\rm SM} \to b\bar{b})}, \tag{3.1}$$

$$\mu_{\tau\tau} = \frac{\sigma_{\rm 2HDM}(gg \to \phi)}{\sigma_{\rm SM}(gg \to h_{\rm SM})} \times \frac{\mathcal{BR}_{\rm 2HDM}(\phi \to \tau\tau)}{\mathcal{BR}_{\rm SM}(h_{\rm SM} \to \tau\tau)} = |c_{\phi tt}|^2 \times \frac{\mathcal{BR}_{\rm 2HDM}(\phi \to \tau\tau)}{\mathcal{BR}_{\rm SM}(h_{\rm SM} \to \tau\tau)}, \tag{3.2}$$

$$\mu_{\gamma\gamma} = \frac{\sigma_{\rm 2HDM}(gg \to \phi)}{\sigma_{\rm SM}(gg \to h_{\rm SM})} \times \frac{\mathcal{BR}_{\rm 2HDM}(\phi \to \gamma\gamma)}{\mathcal{BR}_{\rm SM}(h_{\rm SM} \to \gamma\gamma)} = |c_{\phi tt}|^2 \times \frac{\mathcal{BR}_{\rm 2HDM}(\phi \to \gamma\gamma)}{\mathcal{BR}_{\rm SM}(h_{\rm SM} \to \gamma\gamma)}, \tag{3.3}$$

where $c_{\phi ZZ}$ and $c_{\phi tt}$ are the ϕ couplings to ZZ and $t\bar{t}$ (entering the LEP and LHC production modes, respectively) normalised to the corresponding SM values. In the present context, ϕ

[5] We have explicitly checked that in the region satisfying the flavour physics constraints, the allowed values of $\sin(\beta-\alpha)$ and χ^{33}_d lead to a reduction of $|c_{\phi bb}|$ when compared to $|c_{\phi tt}|$, so that the contribution from the bottom-quark loop is negligible (nearly 2%).

JHEP05(2024)209

denotes the light CP-even Higgs scalar h and our focus is exclusively on its contributions to the signal. We do not consider the pseudoscalar state A for the explanation of these excesses in this analysis since for a CP-conserving scenario such as ours, the AZZ coupling is forbidden at tree level, rendering the explanation of the LEP excess with a CP-odd state impossible. The experimental measurements for the three signal strengths are expressed as [26, 27, 29]:[6]

$$\mu_{\gamma\gamma}^{\rm exp} = \mu_{\gamma\gamma}^{\rm ATLAS+CMS} = 0.24^{+0.09}_{-0.08}, \qquad \mu_{\tau\tau}^{\rm exp} = 1.2 \pm 0.5, \qquad \mu_{b\bar{b}}^{\rm exp} = 0.117 \pm 0.057, \tag{3.4}$$

where $h_{\rm SM}$ corresponds to a SM-like Higgs boson with a mass of 95 GeV — the mass of the h state of our interest from the 2HDM Type-III. In our analysis, we have combined the di-photon measurements from the ATLAS and CMS experiments, denoted as $\mu_{\gamma\gamma}^{\rm ATLAS}$ and $\mu_{\gamma\gamma}^{\rm CMS}$, respectively. The ATLAS measurement yields a central value of 0.18±0.1 [29] while the CMS measurement yields a central value of $0.33^{+0.19}_{-0.12}$ [27]. By doing so, we aimed at leveraging the strengths of both experiments and improve the precision of our analysis. The combined measurement, denoted as $\mu_{\gamma\gamma}^{\rm ATLAS+CMS}$, is determined by taking the average of the central values without assuming any correlation between them. To evaluate the combined uncertainty we sum ATLAS and CMS uncertainties in quadrature.

To determine whether a simultaneous fit to the observed excesses is possible, a χ^2 analysis is performed using measured central values $\mu^{\rm exp}$ and the 1σ uncertainties $\Delta\mu^{\rm exp}$ of the signal rates related to the two excesses as defined in eqs. (3.1)–(3.3). The contribution to the χ^2 value for each channel ($\gamma\gamma$, $\tau\tau$, $b\bar{b}$) is calculated using the formula

$$\chi^2_{\gamma\gamma,\tau\tau,b\bar{b}} = \frac{\left(\mu_{\gamma\gamma,\tau\tau,b\bar{b}} - \mu^{\rm exp}_{\gamma\gamma,\tau\tau,b\bar{b}}\right)^2}{\left(\Delta\mu^{\rm exp}_{\gamma\gamma,\tau\tau,b\bar{b}}\right)^2}. \tag{3.5}$$

So, the resulting χ^2 which we will use to judge whether the points from the model describe the excess in three channels, reads as:

$$\chi^2_{\gamma\gamma+\tau\tau+b\bar{b}} = \chi^2_{\gamma\gamma} + \chi^2_{\tau\tau} + \chi^2_{b\bar{b}}. \tag{3.6}$$

4 Theoretical and experimental constraints

In our study we use a comprehensive set of theoretical and experimental constraints that must be satisfied to establish a viable model.

4.1 Theoretical constraints

In our study we impose the following set of the theoretical constraints on the scalar potential.

- **Unitarity.** The scattering processes involving (pseudo)scalar-(pseudo)scalar, gauge-gauge and/or (pseudo)scalar-gauge initial and/or final states must satisfy unitarity constraints. The eigenvalues e_i of the tree-level 2-to-2 body scattering matrix should meet the following criteria: $|e_i| < 8\pi$ [40, 41].

[6] The value of $\mu_{\gamma\gamma}^{\rm exp}$ which we have decided to take form the latest version of [29] approximately agrees with our rough estimation which we have found to be about 0.3.

JHEP05(2024)209

- **Perturbativity.** Adherence to perturbativity constraints imposes an upper limit on the quartic couplings of the Higgs potential: $|\lambda_i| < 8\pi$ [5].

- **Vacuum Stability.** The scalar potential must be positive and bounded from below in any direction of the fields Φ_i to ensure vacuum stability. This requires that $\lambda_1 > 0$, $\lambda_2 > 0$, $\lambda_3 > -\sqrt{\lambda_1\lambda_2}$, and $\lambda_3 + \lambda_4 - |\lambda_5| > -\sqrt{\lambda_1\lambda_2}$ [42, 43].

4.2 Experimental constraints

We also apply a variety of experimental constraints from EW Precision Observables (EWPOs), measurements of the observed Higgs boson properties at the LHC, lack of signals from non-SM-like Higgs bosons at LEP, Tevatrron and LHC as well as flavour observables, which include the following.

- **EWPOs.** We require a 95% C.L. in matching the global fit results of the EW oblique parameters S, T and U [44, 45] with the following values [46]:

$$S = 0.05 \pm 0.08, \quad T = 0.09 \pm 0.07, \quad \rho_{ST} = 0.92 \quad (\text{for } U = 0).$$

- **SM-like Higgs Boson Discovery.** We made sure that the points from our parameter space agree with the experimental measurement of the properties of the discovered SM-like Higgs boson with mass of $\approx 125\,\text{GeV}$ red at 95% C.L. To do this we have used the public code `HiggsSignals-3` [47, 48] via `HiggsTools` [49] to perform a χ^2 test in order to check how the Higgs signal strengths from Tevatron and LHC are compatible with the model predictions.

- **Non-SM-like Higgs Boson Exclusions.** To further scrutinise the parameter space of our 2HDM Type-III, we subject the selected parameter space points to rigorous examinations against exclusion limits derived from additional Higgs boson searches. We utilise the code `HiggsBounds-6` [50–53] via `HiggsTools` to incorporate the exclusion constraints from various experiments, including LEP, Tevatron and the LHC.

- ***B*-Physics Observables.** We test various B-physics observables against experimental data using the public code `SuperIso_v4.1` [54]. The following experimental measurements are used in our analysis:

  By rigorously examining these B-physics observables against experimental constraints, we can validate the compatibility of our 2HDM Type-III with existing data and potentially uncover any deviations that could indicate new physics phenomena.

5 Explanation of the excesses

In this section, we present our numerical analysis of the 2HDM Type-III parameter space. For the 2HDM Type-III spectrum generation, we have employed `2HDMC 1.8.0`[60], which considers the theoretical constraints discussed in the previous section, along with the electroweak precision observables (EWPOs). Subsequently, we validate our results by comparing them to Higgs data, utilizing `HiggsTools` [49], which includes the most recent versions of

JHEP05(2024)209

Observable	Value	Reference
$\mathcal{BR}(\overline{B} \to X_s\gamma)\vert_{E_\gamma<1.6\text{ GeV}}$	$(3.32 \pm 0.15) \times 10^{-4}$	[55]
$\mathcal{BR}(B^+ \to \tau^+\nu_\tau)$	$(1.06 \pm 0.19) \times 10^{-4}$	[55]
$\mathcal{BR}(D_s \to \tau\nu_\tau)$	$(5.51 \pm 0.18) \times 10^{-2}$	[55]
$\mathcal{BR}(B_s \to \mu^+\mu^-)$ (LHCb)	$\left(3.09^{+0.46}_{-0.43}\right) \times 10^{-9}$	[56, 57]
$\mathcal{BR}(B_s \to \mu^+\mu^-)$ (CMS)	$\left(3.83^{+0.38}_{-0.36}\right) \times 10^{-9}$	[58]
$\mathcal{BR}(B^0 \to \mu^+\mu^-)$ (LHCb)	$\left(1.2^{+0.8}_{-0.7}\right) \times 10^{-10}$	[56, 57]
$\mathcal{BR}(B^0 \to \mu^+\mu^-)$ (CMS)	$\left(0.37^{+0.75}_{-0.67}\right) \times 10^{-10}$	[58]
$\mathcal{BR}(K \to \mu\nu_\mu)/\mathcal{BR}(\pi \to \mu\nu_\mu)$	0.6357 ± 0.0011	[59]

Table 2. Flavour physics observables and corresponding values employed in our analysis.

m_h	m_H	m_A	$m_{H^\pm}$	$s_{\beta-\alpha}$	$\tan\beta$	m_{12}^2	$\chi_{ij}^{f,\ell}$
[94; 97]	125.09	[80; 300]	[160; 200]	$[-0.5; 0]$	[1; 30]	$m_h^2 \tan\beta/(1+\tan^2\beta)$	$[-3; 3]$

Table 3. Scan ranges of the 2HDM Type-III input parameters. Masses are given in GeV.

both `HiggsBounds` and `HiggsSignals`. In accordance with the above discussions, we consider the scenario where the heavier CP-even Higgs boson H is the SM-like Higgs particle $H_{\rm SM}$ discovered at the LHC with $m_{H_{\rm SM}} \approx 125\,\text{GeV}$. In this scenario the lighter CP-even Higgs, h, is the source of the observed excess in $\gamma\gamma$, $\tau\tau$ and $b\bar{b}$ channels around 95 GeV, which we previously labelled as $h_{\rm SM}$. To explore this scenario, we conducted a systematic random scan across the parameter ranges specified in table 3.[7]

We then investigate parameter spaces that satisfy the condition $\chi^2_{125} \leq 189.4$, corresponding to a 95% Confidence Level (C.L.) for 159 degrees of freedom, where χ^2_{125} corresponds to the χ^2 evaluated by `HiggsSignals` for the 125 GeV Higgs signal strength measurements. Subsequently, we examine 2-dimensional (2D) planes of the signal strength parameters: $(\mu_{\gamma\gamma} - \mu_{\tau\tau})$, $(\mu_{\gamma\gamma} - \mu_{b\bar{b}})$ and $(\mu_{b\bar{b}} - \mu_{\tau\tau})$.

In the following we will refer to the h and H states of the 2HDM Type-III by using the labels 'h_{95}' and 'h_{125}', respectively. In figure 1, we present the results for $\chi^2_{\gamma\gamma+\tau\tau+b\bar{b}}$ in the form of its colour map projected into the $(\mu_{\tau\tau}$-$\mu_{\gamma\gamma})$ (left), $(\mu_{b\bar{b}}$-$\mu_{\gamma\gamma})$ (middle) and $(\mu_{\tau\tau}$-$\mu_{b\bar{b}})$ (right) planes of the signal strength parameters. The dashed ellipses define the regions consistent with the excess at 1σ described by the $\chi^2_x + \chi^2_y = 2.30$ equation, where the subscripts x and y label each possible pairing out of three signal channels ($\gamma\gamma$, $\tau\tau$ and $b\bar{b}$), depending on the frame of figure 1. The black, gray and red contours are for the χ^2 constructed using the $\mu_{\gamma\gamma}^{\rm CMS}$, $\mu_{\gamma\gamma}^{\rm ATLAS}$ and $\mu_{\gamma\gamma}^{\rm CMS+ATLAS}$ signal strengths, respectively. The value of $\chi^2_{\gamma\gamma+\tau\tau+b\bar{b}}$ is indicated by the vertical colourmap. The grey points represent exclusions based on recent CMS searches[8] [61] for the production of a Higgs boson in association with

[7] In this work, we do not include the contributions to the signal from the CP-odd state.

[8] This limit has not yet been integrated into `HiggsBounds-6`.

JHEP05(2024)209

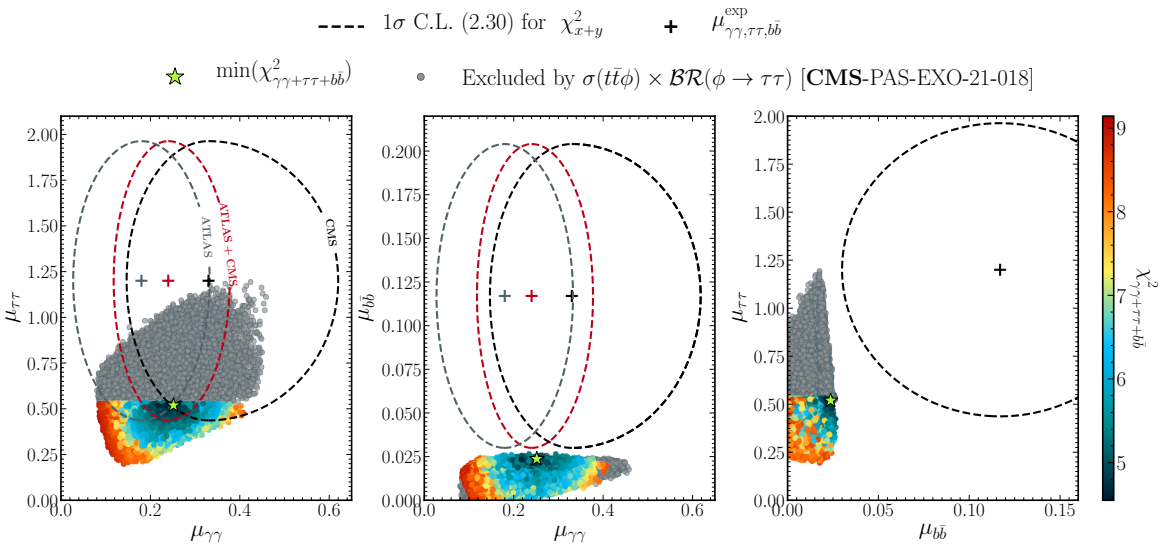

Figure 1. The colour map of $\chi^2_{\gamma\gamma+\tau\tau+b\bar{b}}$ in the $(\mu_{\gamma\gamma}-\mu_{\tau\tau})$, $(\mu_{\gamma\gamma}-\mu_{b\bar{b}})$ and $(\mu_{b\bar{b}}-\mu_{\tau\tau})$ planes of the signal strength parameters for 2HDM Type-III parameter space under study. The ellipses define the regions consistent with the excess at 1σ C.L. The contribution from $\mu_{\gamma\gamma}$ to χ^2 for black, gray and red contours comes from CMS, ATLAS and combined CMS+ATLAS data respectively. As detailed in the text, the contribution to χ^2 from $\mu_{\tau\tau}$ (left frame) comes from CMS data while the contribution from $\mu_{b\bar{b}}$ (middle frame) comes from LEP data. Grey points are excluded by $\sigma(tt\phi)\times\mathcal{BR}(\phi\to\tau\tau)$ [61]. The position of $\chi^2_{95\rm min}$ is marked by a green star.

either a top-quark pair or a Z boson, with the subsequent decay into a tau pair. The green star, indicating the position of $\chi^2_{95,\rm min}$ which is the minimum of $\chi^2_{\gamma\gamma+\tau\tau+b\bar{b}}$, has a value of 4.55, corresponds to a 1.26 σ C.L. for three degrees of freedom even though this minimum lies solely within the 1σ C.L. contour for the $\mu_{\tau\tau}$-$\mu_{\gamma\gamma}$ pair of signal strengths and not for the other pairs. Furthermore, numerous points surrounding $\chi^2_{95,\rm min}$ depicted by the dark blue colour indicating the capability of the 2HDM Type-III to explain the observed excess across all three channels simultaneously at 1.5σ C.L or better reaching up to about 1.3σ.

One can also note from the middle and the right frames of figure 1 that all points are situated outside of the 1σ ellipses because it is difficult to achieve large enough values of $\mu_{b\bar{b}}$ satisfying the three constraints simultaneously. This happens because the $\gamma\gamma$ excess is achieved via enhancement of $\mathcal{BR}(h_{95}\to\gamma\gamma)$ due to the decrease of $\Gamma_{b\bar{b}}$ (the main channel of h_{95} decay) and the respective decrease of $\mathcal{BR}(h_{95}\to b\bar{b})$.

In figure 2, we show $\chi^2_{\gamma\gamma+\tau\tau+b\bar{b}}$ in our parameter scans as a function of $s_{\beta-\alpha}$. We also indicate the value of the Higgs couplings to SM gauge bosons, $|c_{h_{125}VV}|$ (left) and $|c_{h_{125}\gamma\gamma}|$,[9] (right) in the colour bar. The horizontal dashed(dash-dot) line represents the $1\sigma(2\sigma)$ region corresponding to the three excesses ($\gamma\gamma$, $\tau\tau$, $b\bar{b}$). Clearly one can read from the left panel that, when simultaneously describing the three excesses at 1.3σ C.L., the SM-like Higgs coupling to vector bosons $|c_{h_{125}VV}|$ which is proportional to $c_{\beta-\alpha}$ lie close to ~ 1, In contract the coupling to $\gamma\gamma$ exhibits a slight deviation from the predicted SM value, reaching a minimum of 0.91 and a maximum of 0.96.

[9]The normalised coupling for the loop-induced channel $h\to\gamma\gamma$ is defined by $|c_{h\to\gamma\gamma}|^2\equiv\frac{\Gamma(h\to\gamma\gamma)^{\rm 2HDM}}{\Gamma(h\to\gamma\gamma)^{\rm SM}}$.

JHEP05(2024)209

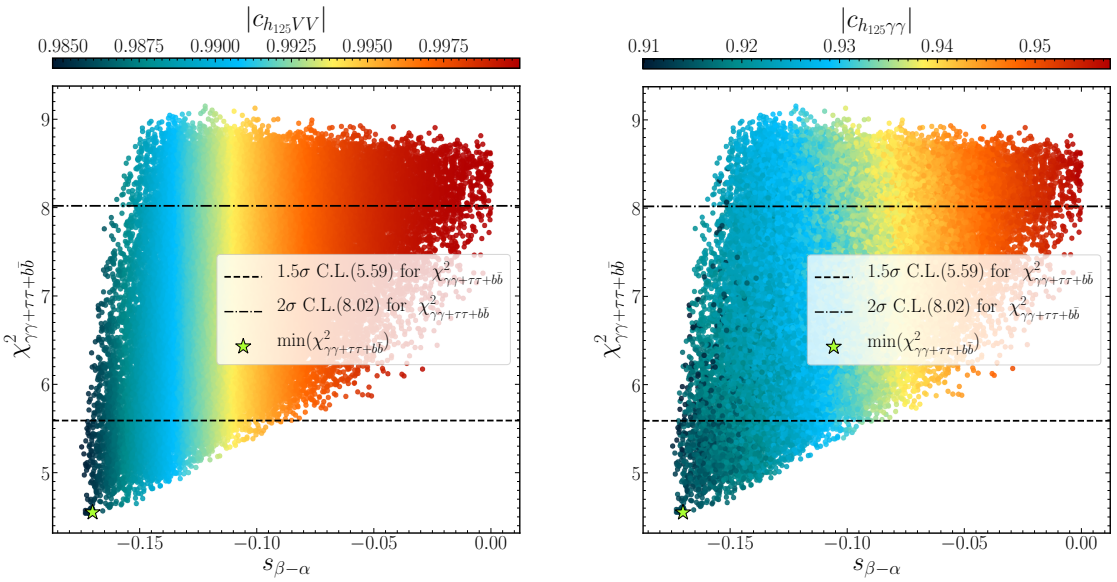

Figure 2. The $\chi^2_{\gamma\gamma+\tau\tau+b\bar{b}}$ dependence upon $s_{\beta-\alpha}$. The colour bar indicates the value of $|c_{h_{125}VV}|$ (left) and $|c_{h_{125}\gamma\gamma}|$ (right). The horizontal dashed(dash-dot) line represents the $1.5\sigma(2\sigma)$ region.

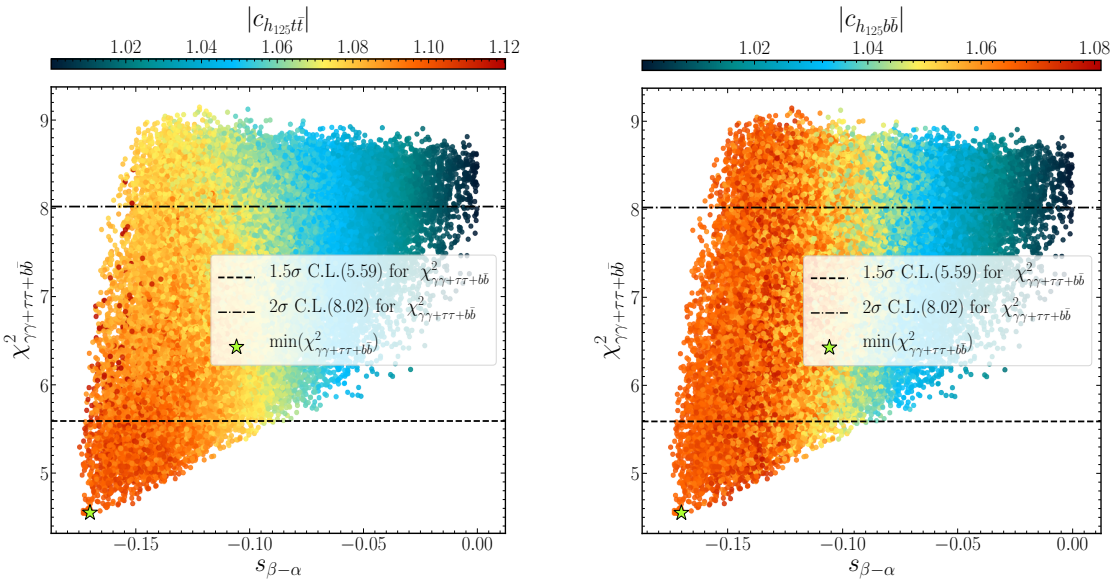

Figure 3. As in figure 2, but the colour coding indicates the value of $|c_{h_{125}t\bar{t}}|$ (left) and $|c_{h_{125}b\bar{b}}|$ (right).

Figure 3 presents analogous plots to those displayed in figure 2. However, in this case, the colour bar represents the values of the couplings of the $\approx 125\,\text{GeV}$ Higgs state to $t\bar{t}$ (left) and to $b\bar{b}$ (right). The explanation of the three excesses simultaneously requires an enhancement of up to 12% and 8% in $c_{h_{125}t\bar{t}}$ and $c_{h_{125}b\bar{b}}$, respectively. The reason for the enhancement in $c_{h_{125}t\bar{t}}$ can be understood as follows. The requirement of fitting the three excesses at 1.3σ C.L. restricts $\sin(\beta-\alpha)$ in the range $\approx$ [-0.18,-0.13]. This makes the s_α/s_β term in the $c_{h_{125}t\bar{t}}$ coupling (see second row, table 1) slightly larger than one. The χ^u_{33} parameter in the second term is constrained by flavour physics to be both small and negative, making

JHEP05(2024)209

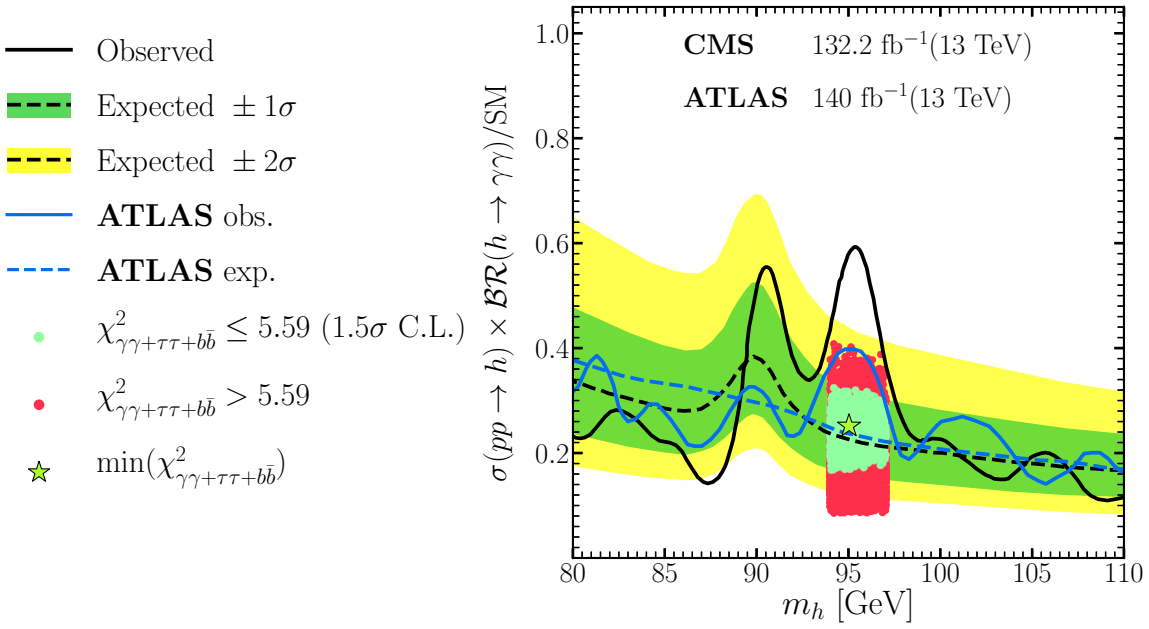

Figure 4. Allowed points, following the discussed theoretical and experimental constraints, superimposed onto the results of the CMS 13 TeV low-mass $\gamma\gamma$ [7] analysis. (Notably, the plot further includes the depiction of the ATLAS expected and observed limits from [8], showcased in blue.) The light green colour represents the parameter points that fit the excesses within a three-dimensional C.L. of 1.5σ ($\chi^2_{95} \leq 5.59$) or better, reaching up to 1.3σ, whereas the points that fit the excesses at 2σ or more are shown in red.

the contribution from the second term minimal. In contrast, the enhancement in $c_{h_{125}b\bar{b}}$ originates from both terms, as χ^d_{33} is larger, contributing substantially to the coupling. A typical set of values for the χ^f_{ij} parameters can be found in table 4 where we describe the features of our best fit point. The implications of the enhancements, in particular in the $c_{h_{125}t\bar{t}}$ coupling, will be discussed subsequently.

In figure 4, we directly compare our allowed parameter points to the experimental data by superimposing these onto the CMS 13 TeV low-mass $\gamma\gamma$ [7] analysis data. The light green colour represents the parameter points that fit the excesses within a three-dimensional C.L. from 1.5σ up to 1.3σ, whereas the points that fit the excesses at 2σ or more are shown in red. It can be clearly observed from the plots that our parameter points are exactly suited to satisfy the excesses.

Figure 5 depicts the correlation between the normalised couplings of the ≈ 125 GeV Higgs using the same color scheme detailed in figure 4. One can see from the plots that the explanation of the three excesses in $b\bar{b}$, $\tau\tau$ and $\gamma\gamma$ channels requires an enhancement of the $h_{125}t\bar{t}$ and $h_{125}b\bar{b}$ couplings deviating by $\sim 11.5\%$ from the SM for $t\bar{t}$ and by $\sim 8\%$ for $b\bar{b}$. In contrast, a decrease can be seen in the Higgs coupling to $\tau\tau$ ($c_{h_{125}\tau\tau}$), deviating from the SM value by about 11%. Furthermore, the plot includes green dashed lines representing the current 1σ uncertainties of the normalised couplings $c_{h_{125}i\bar{j}}$, as measured by CMS [62]. Additionally, orange and blue ellipses are depicted, illustrating the projected experimental precision for the normalised couplings at the HL-LHC [63] with an integrated luminosity of

JHEP05(2024)209

$3000\,\text{fb}^{-1}$ and the projected precision from a combination of data from the HL-LHC and ILC 500, respectively. One should bear in mind that the center of these experimental projections, for HL-LHC and ILC 500, corresponds to the SM value represented by black diamonds. Clearly, each point that simultaneously describes the three excesses is situated outside the ellipses corresponding to the HL-LHC and ILC 500. Since the points deviate significantly from the SM predictions, the expected precision of the HL-LHC and ILC 500 experiments would allow us to distinguish between the SM-like properties of h_{125} and the H from the 2HDM Type-III model within the parameter range that aligns with the observed excesses. Moreover, one can see that already at the HL-LHC one will be able either to discover or rule out the scenario which describes the current excess in three channels under study.

Figure 6 illustrates the allowed parameter space in the 2HDM Type-III satisfying theoretical and experimental constraints in the $(m_h, \sigma_{tth_{125}}/\sigma_{tth}^{\text{SM}})$ plane. The black dashed line corresponds to the observed value from CMS [62] and the lime green (yellow) band represents instead the 1σ (2σ) range. The hatched area denotes the 95% C.L. probability sensitivity of the HL-LHC [63] to the normalised cross section $\sigma_{tth_{125}}/\sigma_{tth}^{\text{SM}}$, centered on the SM value (solid red line). It is evident from the figure that all the points that simultaneously explain the three excesses at 1.5σ C.L or better. represented by the light green colour, fall within the 2σ measurement range of CMS. Additionally, as seen in figure 5, these points exhibit an enhancement in the $h_{125}t\bar{t}$ coupling. In fact, due to such an enhancement, these points deviate significantly from the 2σ level of the HL-LHC projection. Note, however, that the central value used for the HL-LHC measurement corresponds to the SM prediction, i.e., 1. Thus, for points that are notably away from the SM prediction, the projected precision of the HL-LHC experiment would be sufficient to distinguish between the SM-like properties of the h_{125} and the predictions of the 2HDM Type-III within the parameter space consistent with the observed enhancement in the $h_{125}t\bar{t}$ coupling.

In summary, there is a smoking-gun prediction stemming from our 2HDM Type-III scenario, which simultaneously explains $\gamma\gamma, \tau\tau$ and $b\bar{b}$ anomalies at 1.3 σ C.L. and can be tested at the LHC.

On the one hand, $c_{h_{125}t\bar{t}}$ and $c_{h_{125}b\bar{b}}$ are consistently larger than 1, while $c_{h_{125}\tau\tau}$ is consistently smaller than 1. Among these couplings, $c_{h_{125}t\bar{t}}$ can be precisely measured in various production modes, not only in gluon-gluon fusion where, however, there is contamination from b-quark loops, but also in associated production with $t\bar{t}$ pairs, which could then be tested at the (HL-)LHC, via $pp \to t\bar{t}h_{125}$, and an ILC 500, via $e^+e^- \to t\bar{t}h_{125}$.

Finally, we conclude this section by providing a detailed overview of our best fit point in table 4. One can observe from table 4 that the best fit point features a small negative value for the χ_{33}^u parameter. This, in combination with the small negative $\sin(\beta-\alpha)$ values preferred in our parameter scan gives rise to the observed enhancement in the $h_{125}t\bar{t}$ couplings (see table 1).

JHEP05(2024)209

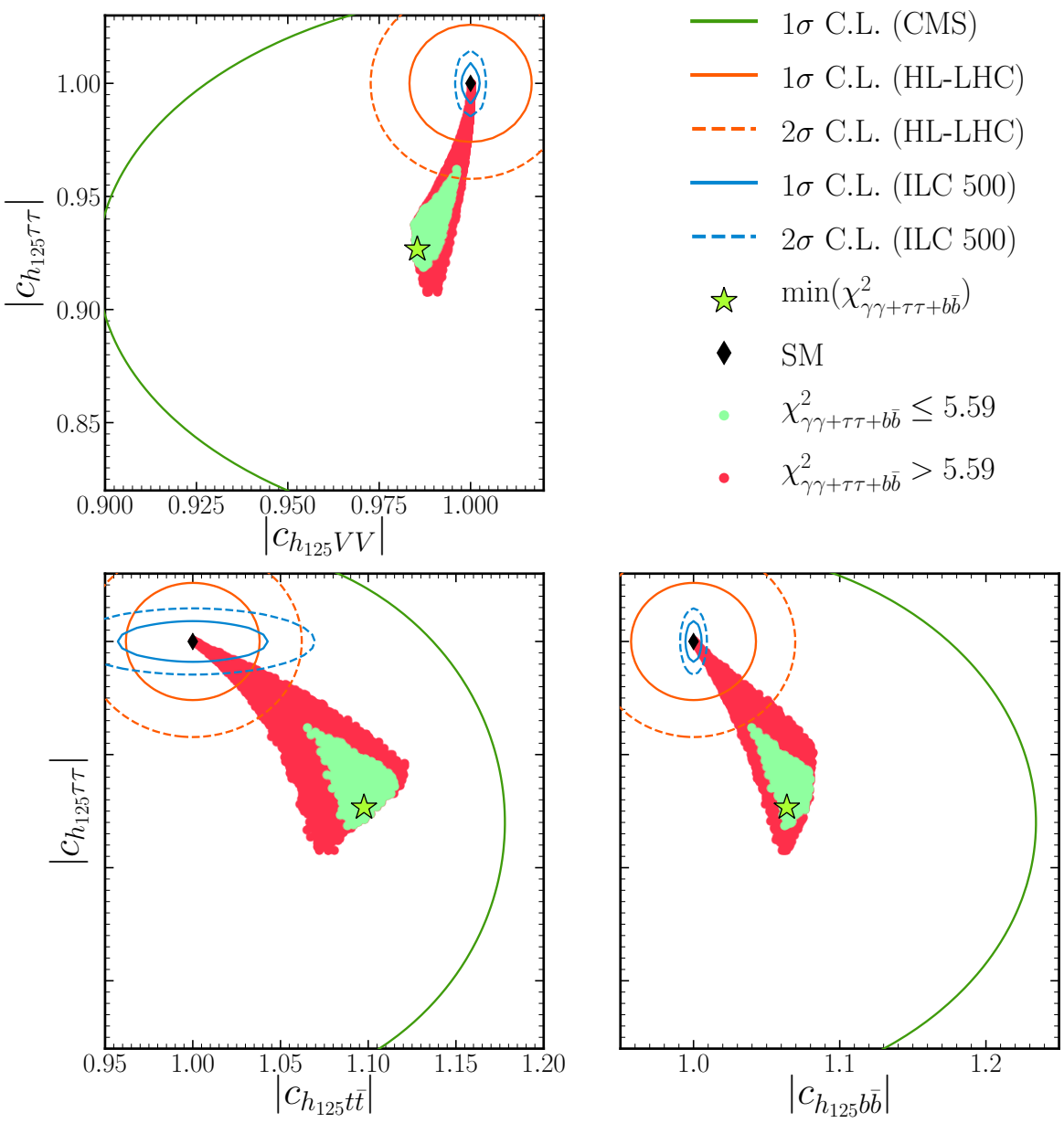

Figure 5. Correlations between the normalized couplings $|c_{h_{125}\tau\tau}|$, $|c_{h_{125}VV}|$, $|c_{h_{125}t\bar{t}}|$, and $|c_{b_{125}t\bar{b}}|$, with colours corresponding to those in figure 4, are illustrated. Also presented are the current 1σ uncertainties of the coupling coefficients' measurements from CMS [62], depicted by green dashed lines. The orange and blue ellipses indicate the projected uncertainties at the HL-LHC [63], and following a combination of data from both the HL-LHC and the ILC at a center-of-mass energy of 500 GeV [64], respectively.

JHEP05(2024)209

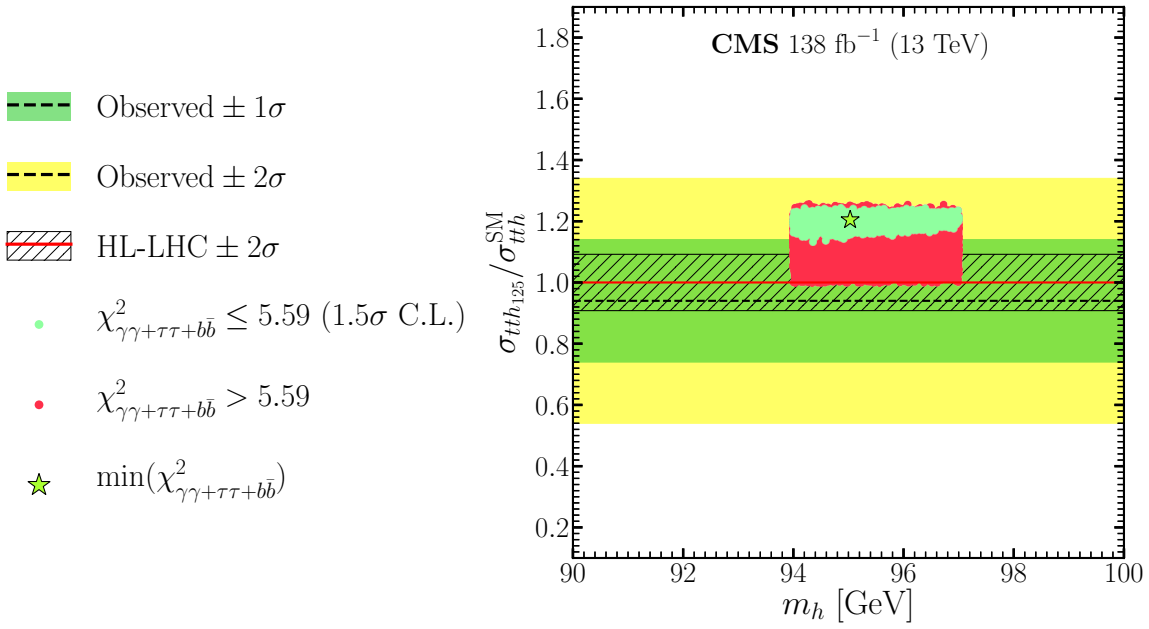

Figure 6. Predicted signal strength $\sigma_{tth_{125}}/\sigma^{SM}_{tth}$ in relation to the three observed excesses. The black dashed line represents the observed value from CMS [62] while the lime green (yellow) band denotes the 1.5σ (2σ) range around the observed value. The hatched area illustrates the 95% probability sensitivity of the HL-LHC [63] to the normalised cross section $\sigma_{tth_{125}}/\sigma^{SM}_{tth}$, centred on the value of the SM (depicted as a solid red line). The colours correspond to those in figure 4.

6 Conclusions

To date, large data samples have been accumulated by the LHC experiments and many analyses have been performed to examine the discussed 95 GeV excesses, following initial observations. In order to better explain the nature of these potential anomalies, a careful examination of the data, in-depth simulations and advanced computational approaches have been carried out in the literature. Along these lines, we have in this article proposed a theoretical framework, the 2HDM Type-III with a specific Yukawa texture, as a possible solution to the $\gamma\gamma$, $\tau\tau$ and $b\bar{b}$ anomalies. Specifically, we concentrated on a Higgs boson with a mass of about 95 GeV produced by gluon-gluon fusion at the 13 TeV LHC and decaying into $\tau\tau$ and $\gamma\gamma$ as well as produced by Higgs-strahlung at LEP and decaying into $b\bar{b}$.

By assuming that the heaviest CP-even Higgs state, H, is the one discovered at the LHC with mass ≈ 125 GeV, we have identified parameter space regions where the lightest CP-even state, h, with a mass of ≈ 95 GeV, can explain simultaneously the observed excesses through a χ^2 analysis at approximately 1.3 σ C.L. while accommodating both standard theoretical requirements of self-consistency and up-to-date experimental constraints.

Throughout this paper, we have analysed correlations amongst the signal strengths $\mu_{\gamma\gamma}$, $\mu_{\tau\tau}$ and $\mu_{b\bar{b}}$ at 1σ level, arguing that the results presented are compelling and support a more extensive investigation of the proposed 2HDM Type-III scenario, by looking at processes predicted therein, which would constitute an hallmark signature of it, like $pp \to t\bar{t}H$

JHEP05(2024)209

production, at both Run 3 of the LHC and the HL-LHC, which would be significantly enhanced with respect to the SM yield.

In fact, also the study of $e^+e^- \to t\bar{t}H$ at the ILC 500, which would probe the coupling of H to top (anti)quarks at the percent level, will play a crucial role in confirming the BSM construct pursued in our investigation. Thus, by incorporating the insights gained from these complementary measurements, a more comprehensive understanding of the nature of the studied excesses and the underlying theoretical framework can be achieved (assuming their persistence in future data samples at these machines).

Moreover, the anticipated precision of the HL-LHC and ILC 500 allows for effective differentiation between the SM-like characteristics of the H state and the predictions of the 2HDM Type-III. This distinction is achievable for data points that display notable deviations from the SM predictions, while remaining within the parameter space that corresponds to the observed enhancement in the $t\bar{t}H$ coupling. Finally, one should stress that the precise measurement of the $t\bar{t}H$ coupling would be also very instrumental for discovery or dismissal of the proposed scenario already in the near future at the HL-LHC.

To aid such investigations, we have presented the details of our best fit point for further phenomenological studies in these directions.

Acknowledgments

AB and SM are supported in part through the NExT Institute and STFC CG ST/L000296/1. AB would like to thank Prof. Glen Cowan for discussions around the statistical aspects of our study. The work of RB and MB is supported by the Moroccan Ministry of Higher Education and Scientific Research MESRSFC and CNRST Project PPR/2015/6. MB acknowledges the use of CNRST/HPC-MARWAN in completing this work. SS is supported in full by the NExT Institute.

Parameters	★
(Masses are in GeV)	
m_h	95.03
m_H	125.09
m_A	94.77
$m_{H^\pm}$	162.95
$\tan\beta$	1.74
$\sin(\beta-\alpha)$	−0.17
χ^u_{11}	0.02
χ^u_{22}	0.54
χ^u_{33}	−0.08
χ^d_{11}	−0.41
χ^d_{22}	0.24
χ^d_{33}	1.55
χ^ℓ_{11}	−0.06
χ^ℓ_{22}	0.33
χ^ℓ_{33}	0.97
Effective coupling $c_{h_{125}i\bar{i}}$	
$c_{h_{125}t\bar{t}}$	1.10
$c_{h_{125}b\bar{b}}$	1.06
$c_{h_{125}\tau\tau}$	0.92
Collider signal strength	
$\mu_{\gamma\gamma}$	0.25
$\mu_{\tau\tau}$	0.51
$\mu_{b\bar{b}}$	0.02
Total decay width in MeV	
$\Gamma(h)$	0.27
$\Gamma(H)$	4.73
$\Gamma(A)$	0.66
$\Gamma(H^\pm)$	4.77
$\mathcal{BR}(h\to XY)$ in %	
$\mathcal{BR}(h\to\gamma\gamma)$	0.15
$\mathcal{BR}(h\to gg)$	13.82
$\mathcal{BR}(h\to b\bar{b})$	65.37
$\mathcal{BR}(h\to c\bar{c})$	—
$\mathcal{BR}(h\to s\bar{s})$	0.50
$\mathcal{BR}(h\to\mu^+\mu^-)$	0.67
$\mathcal{BR}(h\to\tau\tau)$	19.33
$\mathcal{BR}(h\to ZZ)$	—
$\mathcal{BR}(h\to W^+W^-)$	0.12
$\mathcal{BR}(H\to XY)$ in %	
$\mathcal{BR}(H\to\gamma\gamma)$	0.16
$\mathcal{BR}(H\to gg)$	8.16
$\mathcal{BR}(H\to b\bar{b})$	64.08
$\mathcal{BR}(H\to c\bar{c})$	3.07
$\mathcal{BR}(H\to\tau\tau)$	4.70
$\mathcal{BR}(H\to ZZ)$	2.19
$\mathcal{BR}(H\to W^+W^-)$	17.48
$\mathcal{BR}(A\to XY)$ in %	
$\mathcal{BR}(A\to\gamma\gamma)$	0.046
$\mathcal{BR}(A\to gg)$	28.70
$\mathcal{BR}(A\to b\bar{b})$	66.95
$\mathcal{BR}(A\to c\bar{c})$	0.40
$\mathcal{BR}(A\to\mu\mu)$	0.16
$\mathcal{BR}(A\to\tau\tau)$	3.53
$\mathcal{BR}(H^\pm\to XY)$ in %	
$\mathcal{BR}(H^\pm\to cs)$	0.11
$\mathcal{BR}(H^\pm\to W^+h)$	33.79
$\mathcal{BR}(H^\pm\to W^+A)$	35.62
$\mathcal{BR}(H^\pm\to\tau\nu)$	0.84
$\mathcal{BR}(H^\pm\to tb)$	29.47

Table 4. The full description of the best fit point $\chi^2_{95,\min}$ (green star).

JHEP05(2024)209

References

[1] ATLAS collaboration, *Observation of a new particle in the search for the Standard Model Higgs boson with the ATLAS detector at the LHC*, *Phys. Lett. B* **716** (2012) 1 [arXiv:1207.7214] [INSPIRE].

[2] CMS collaboration, *Observation of a New Boson at a Mass of 125 GeV with the CMS Experiment at the LHC*, *Phys. Lett. B* **716** (2012) 30 [arXiv:1207.7235] [INSPIRE].

[3] S. Moretti and S. Khalil, *Supersymmetry Beyond Minimality: From Theory to Experiment*, CRC Press (2019) [INSPIRE].

[4] J.F. Gunion, H.E. Haber, G.L. Kane and S. Dawson, *Errata for the Higgs hunter's guide*, hep-ph/9302272 [INSPIRE].

[5] G.C. Branco et al., *Theory and phenomenology of two-Higgs-doublet models*, *Phys. Rept.* **516** (2012) 1 [arXiv:1106.0034] [INSPIRE].

[6] CMS collaboration, *Search for a standard model-like Higgs boson in the mass range between 70 and 110 GeV in the diphoton final state in proton-proton collisions at* $\sqrt{s} = 8$ *and 13 TeV*, *Phys. Lett. B* **793** (2019) 320 [arXiv:1811.08459] [INSPIRE].

[7] CMS collaboration, *Search for a standard model-like Higgs boson in the mass range between 70 and 110 GeV in the diphoton final state in proton-proton collisions at* $\sqrt{s} = 13$ *TeV*, CMS-PAS-HIG-20-002, CERN, Geneva (2023).

[8] C. Arcangeletti, *Measurement of Higgs boson production and search for new resonances in final states with photons and Z bosons, with the ATLAS detector*, https://cds.cern.ch/record/2861392.

[9] ATLAS collaboration, *Search for resonances in the 65 to 110 GeV diphoton invariant mass range using* $80\,fb^{-1}$ *of pp collisions collected at* $\sqrt{s} = 13$ *TeV with the ATLAS detector*, ATLAS-CONF-2018-025, CERN, Geneva (2018).

[10] CMS collaboration, *Searches for additional Higgs bosons and for vector leptoquarks in* $\tau\tau$ *final states in proton-proton collisions at* $\sqrt{s} = 13$ *TeV*, *JHEP* **07** (2023) 073 [arXiv:2208.02717] [INSPIRE].

[11] LEP Working Group for Higgs boson searches et al. collaborations, *Search for the standard model Higgs boson at LEP*, *Phys. Lett. B* **565** (2003) 61 [hep-ex/0306033] [INSPIRE].

[12] ALEPH et al. collaborations, *Search for neutral MSSM Higgs bosons at LEP*, *Eur. Phys. J. C* **47** (2006) 547 [hep-ex/0602042] [INSPIRE].

[13] J. Cao et al., *Diphoton signal of the light Higgs boson in natural NMSSM*, *Phys. Rev. D* **95** (2017) 116001 [arXiv:1612.08522] [INSPIRE].

[14] S. Heinemeyer et al., *Phenomenology of a 96 GeV Higgs boson in the 2HDM with an additional singlet*, *Phys. Rev. D* **106** (2022) 075003 [arXiv:2112.11958] [INSPIRE].

[15] T. Biekötter et al., *Possible indications for new Higgs bosons in the reach of the LHC: N2HDM and NMSSM interpretations*, *Eur. Phys. J. C* **82** (2022) 178 [arXiv:2109.01128] [INSPIRE].

[16] T. Biekötter, M. Chakraborti and S. Heinemeyer, *A 96 GeV Higgs boson in the N2HDM*, *Eur. Phys. J. C* **80** (2020) 2 [arXiv:1903.11661] [INSPIRE].

JHEP05(2024)209

[17] J. Cao et al., *96 GeV diphoton excess in seesaw extensions of the natural NMSSM*, *Phys. Rev. D* **101** (2020) 055008 [arXiv:1908.07206] [INSPIRE].

[18] T. Biekötter, S. Heinemeyer and G. Weiglein, *Excesses in the low-mass Higgs-boson search and the W-boson mass measurement*, *Eur. Phys. J. C* **83** (2023) 450 [arXiv:2204.05975] [INSPIRE].

[19] S. Iguro, T. Kitahara and Y. Omura, *Scrutinizing the 95–100 GeV di-tau excess in the top associated process*, *Eur. Phys. J. C* **82** (2022) 1053 [arXiv:2205.03187] [INSPIRE].

[20] W. Li, H. Qiao and J. Zhu, *Light Higgs boson in the NMSSM confronted with the CMS di-photon and di-tau excesses*, *Chin. Phys. C* **47** (2023) 123102 [arXiv:2212.11739] [INSPIRE].

[21] J.M. Cline and T. Toma, *Pseudo-Goldstone dark matter confronts cosmic ray and collider anomalies*, *Phys. Rev. D* **100** (2019) 035023 [arXiv:1906.02175] [INSPIRE].

[22] T. Biekötter and M.O. Olea-Romacho, *Reconciling Higgs physics and pseudo-Nambu-Goldstone dark matter in the S2HDM using a genetic algorithm*, *JHEP* **10** (2021) 215 [arXiv:2108.10864] [INSPIRE].

[23] A. Crivellin, J. Heeck and D. Müller, *Large $h \to bs$ in generic two-Higgs-doublet models*, *Phys. Rev. D* **97** (2018) 035008 [arXiv:1710.04663] [INSPIRE].

[24] G. Cacciapaglia et al., *Search for a lighter Higgs boson in Two Higgs Doublet Models*, *JHEP* **12** (2016) 068 [arXiv:1607.08653] [INSPIRE].

[25] A.A. Abdelalim, B. Das, S. Khalil and S. Moretti, *Di-photon decay of a light Higgs state in the BLSSM*, *Nucl. Phys. B* **985** (2022) 116013 [arXiv:2012.04952] [INSPIRE].

[26] T. Biekötter, S. Heinemeyer and G. Weiglein, *Mounting evidence for a 95 GeV Higgs boson*, *JHEP* **08** (2022) 201 [arXiv:2203.13180] [INSPIRE].

[27] T. Biekötter, S. Heinemeyer and G. Weiglein, *The CMS di-photon excess at 95 GeV in view of the LHC Run 2 results*, *Phys. Lett. B* **846** (2023) 138217 [arXiv:2303.12018] [INSPIRE].

[28] D. Azevedo, T. Biekötter and P.M. Ferreira, *2HDM interpretations of the CMS diphoton excess at 95 GeV*, *JHEP* **11** (2023) 017 [arXiv:2305.19716] [INSPIRE].

[29] T. Biekötter, S. Heinemeyer and G. Weiglein, *95.4 GeV diphoton excess at ATLAS and CMS*, *Phys. Rev. D* **109** (2024) 035005 [arXiv:2306.03889] [INSPIRE].

[30] R. Benbrik, M. Boukidi, S. Moretti and S. Semlali, *Explaining the 96 GeV Di-photon anomaly in a generic 2HDM Type-III*, *Phys. Lett. B* **832** (2022) 137245 [arXiv:2204.07470] [INSPIRE].

[31] R. Benbrik, M. Boukidi, S. Moretti and S. Semlali, *Probing a 96 GeV Higgs Boson in the Di-Photon Channel at the LHC*, *PoS* **ICHEP2022** (2022) 547 [arXiv:2211.11140] [INSPIRE].

[32] S. Davidson and H.E. Haber, *Basis-independent methods for the two-Higgs-doublet model*, *Phys. Rev. D* **72** (2005) 035004 [*Erratum ibid.* **72** (2005) 099902] [hep-ph/0504050] [INSPIRE].

[33] S.L. Glashow and S. Weinberg, *Natural Conservation Laws for Neutral Currents*, *Phys. Rev. D* **15** (1977) 1958 [INSPIRE].

[34] E.A. Paschos, *Diagonal Neutral Currents*, *Phys. Rev. D* **15** (1977) 1966 [INSPIRE].

[35] T.P. Cheng and M. Sher, *Mass Matrix Ansatz and Flavor Nonconservation in Models with Multiple Higgs Doublets*, *Phys. Rev. D* **35** (1987) 3484 [INSPIRE].

[36] J.L. Diaz-Cruz, R. Noriega-Papaqui and A. Rosado, *Mass matrix ansatz and lepton flavor violation in the THDM-III*, *Phys. Rev. D* **69** (2004) 095002 [hep-ph/0401194] [INSPIRE].

JHEP05(2024)209

[37] J. Hernandez-Sanchez, S. Moretti, R. Noriega-Papaqui and A. Rosado, *Off-diagonal terms in Yukawa textures of the Type-III 2-Higgs doublet model and light charged Higgs boson phenomenology*, *JHEP* **07** (2013) 044 [arXiv:1212.6818] [INSPIRE].

[38] A. Crivellin, A. Kokulu and C. Greub, *Flavor-phenomenology of two-Higgs-doublet models with generic Yukawa structure*, *Phys. Rev. D* **87** (2013) 094031 [arXiv:1303.5877] [INSPIRE].

[39] R. Benbrik, C.-H. Chen and T. Nomura, $h, Z \to \ell_i \bar{\ell}_j$, Δa_μ, $\tau \to (3\mu, \mu\gamma)$ *in generic two-Higgs-doublet models*, *Phys. Rev. D* **93** (2016) 095004 [arXiv:1511.08544] [INSPIRE].

[40] S. Kanemura, T. Kubota and E. Takasugi, *Lee-Quigg-Thacker bounds for Higgs boson masses in a two doublet model*, *Phys. Lett. B* **313** (1993) 155 [hep-ph/9303263] [INSPIRE].

[41] A.G. Akeroyd, A. Arhrib and E.-M. Naimi, *Note on tree level unitarity in the general two Higgs doublet model*, *Phys. Lett. B* **490** (2000) 119 [hep-ph/0006035] [INSPIRE].

[42] A. Barroso, P.M. Ferreira, I.P. Ivanov and R. Santos, *Metastability bounds on the two Higgs doublet model*, *JHEP* **06** (2013) 045 [arXiv:1303.5098] [INSPIRE].

[43] N.G. Deshpande and E. Ma, *Pattern of Symmetry Breaking with Two Higgs Doublets*, *Phys. Rev. D* **18** (1978) 2574 [INSPIRE].

[44] W. Grimus, L. Lavoura, O.M. Ogreid and P. Osland, *A precision constraint on multi-Higgs-doublet models*, *J. Phys. G* **35** (2008) 075001 [arXiv:0711.4022] [INSPIRE].

[45] W. Grimus, L. Lavoura, O.M. Ogreid and P. Osland, *The oblique parameters in multi-Higgs-doublet models*, *Nucl. Phys. B* **801** (2008) 81 [arXiv:0802.4353] [INSPIRE].

[46] Particle Data Group collaboration, *Review of Particle Physics*, *PTEP* **2020** (2020) 083C01 [INSPIRE].

[47] P. Bechtle et al., *HiggsBounds-5: Testing Higgs Sectors in the LHC 13 TeV Era*, *Eur. Phys. J. C* **80** (2020) 1211 [arXiv:2006.06007] [INSPIRE].

[48] P. Bechtle et al., *HiggsSignals-2: Probing new physics with precision Higgs measurements in the LHC 13 TeV era*, *Eur. Phys. J. C* **81** (2021) 145 [arXiv:2012.09197] [INSPIRE].

[49] H. Bahl et al., *HiggsTools: BSM scalar phenomenology with new versions of HiggsBounds and HiggsSignals*, *Comput. Phys. Commun.* **291** (2023) 108803 [arXiv:2210.09332] [INSPIRE].

[50] P. Bechtle et al., *HiggsBounds: Confronting Arbitrary Higgs Sectors with Exclusion Bounds from LEP and the Tevatron*, *Comput. Phys. Commun.* **181** (2010) 138 [arXiv:0811.4169] [INSPIRE].

[51] P. Bechtle et al., *HiggsBounds 2.0.0: Confronting Neutral and Charged Higgs Sector Predictions with Exclusion Bounds from LEP and the Tevatron*, *Comput. Phys. Commun.* **182** (2011) 2605 [arXiv:1102.1898] [INSPIRE].

[52] P. Bechtle et al., HiggsBounds – 4*: Improved Tests of Extended Higgs Sectors against Exclusion Bounds from LEP, the Tevatron and the LHC*, *Eur. Phys. J. C* **74** (2014) 2693 [arXiv:1311.0055] [INSPIRE].

[53] P. Bechtle et al., *Applying Exclusion Likelihoods from LHC Searches to Extended Higgs Sectors*, *Eur. Phys. J. C* **75** (2015) 421 [arXiv:1507.06706] [INSPIRE].

[54] F. Mahmoudi, *SuperIso v2.3: A program for calculating flavor physics observables in Supersymmetry*, *Comput. Phys. Commun.* **180** (2009) 1579 [arXiv:0808.3144] [INSPIRE].

[55] HFLAV collaboration, *Averages of b-hadron, c-hadron, and τ-lepton properties as of summer 2016*, *Eur. Phys. J. C* **77** (2017) 895 [arXiv:1612.07233] [INSPIRE].

JHEP05(2024)209

[56] LHCb collaboration, *Measurement of the $B_s^0 \to \mu^+\mu^-$ decay properties and search for the $B^0 \to \mu^+\mu^-$ and $B_s^0 \to \mu^+\mu^-\gamma$ decays*, *Phys. Rev. D* **105** (2022) 012010 [arXiv:2108.09283] [INSPIRE].

[57] LHCb collaboration, *Analysis of Neutral B-Meson Decays into Two Muons*, *Phys. Rev. Lett.* **128** (2022) 041801 [arXiv:2108.09284] [INSPIRE].

[58] CMS collaboration, *Measurement of the $B_S^0 \to \mu^+\mu^-$ decay properties and search for the $B^0 \to \mu^+\mu^-$ decay in proton-proton collisions at $\sqrt{s} = 13$ TeV*, *Phys. Lett. B* **842** (2023) 137955 [arXiv:2212.10311] [INSPIRE].

[59] LHCb collaboration, *Measurement of the $B_s^0 \to \mu^+\mu^-$ branching fraction and effective lifetime and search for $B^0 \to \mu^+\mu^-$ decays*, *Phys. Rev. Lett.* **118** (2017) 191801 [arXiv:1703.05747] [INSPIRE].

[60] D. Eriksson, J. Rathsman and O. Stal, *2HDMC: Two-Higgs-Doublet Model Calculator Physics and Manual*, *Comput. Phys. Commun.* **181** (2010) 189 [arXiv:0902.0851] [INSPIRE].

[61] CMS collaboration, *Search for dilepton resonances from decays of (pseudo)scalar bosons produced in association with a massive vector boson or top quark anti-top quark pair at $\sqrt{s} = 13$ TeV*, CMS-PAS-EXO-21-018, CERN, Geneva (2022).

[62] CMS collaboration, *A portrait of the Higgs boson by the CMS experiment ten years after the discovery*, *Nature* **607** (2022) 60 [arXiv:2207.00043] [INSPIRE].

[63] M. Cepeda et al., *Report from Working Group 2: Higgs Physics at the HL-LHC and HE-LHC*, *CERN Yellow Rep. Monogr.* **7** (2019) 221 [arXiv:1902.00134] [INSPIRE].

[64] P. Bambade et al., *The International Linear Collider: A Global Project*, arXiv:1903.01629 [INSPIRE].

JHEP05(2024)209